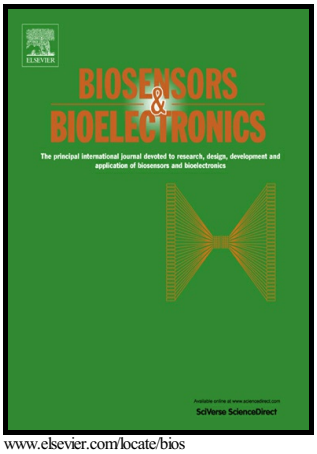

www.elsevier.com/locate/bios

A sensitive sandwich-type immunosensor for the detection of galectin-3 based on N-GNRs-Fe-MOFs@AuNPs nanocomposites and a novel AuPt-Methylene blue nanorod

Zhiyong Tang, Junlin He, Jun Chen, Yazhen Niu, Yilin Zhao, Yuchan Zhang, Chao Yu

PII: S0956-5663(17)30694-2
DOI: https://doi.org/10.1016/j.bios.2017.10.026
Reference: BIOS10051

To appear in: *Biosensors and Bioelectronic*

Received date: 27 July 2017
Revised date: 29 September 2017
Accepted date: 13 October 2017

Cite this article as: Zhiyong Tang, Junlin He, Jun Chen, Yazhen Niu, Yilin Zhao, Yuchan Zhang and Chao Yu, A sensitive sandwich-type immunosensor for the detection of galectin-3 based on N-GNRs-Fe-MOFs@AuNPs nanocomposites and a novel AuPt-Methylene blue nanorod, *Biosensors and Bioelectronic,* https://doi.org/10.1016/j.bios.2017.10.026

A sensitive sandwich-type immunosensor for the detection of galectin-3 based on N-GNRs-Fe-MOFs@AuNPs nanocomposites and a novel AuPt-Methylene blue nanorod

Zhiyong Tang[1], Junlin He[1], Jun Chen, Yazhen Niu, Yilin Zhao, Yuchan Zhang, Chao Yu*

College of Pharmacy, School of public health and management, and Chongqing pharmacodynamic evaluation engineering technology research center, Chongqing Medical University, Chongqing 400016, P.R. China

[1] Junlin He and Zhiyong Tang contributed equally to this work.

*Corresponding author: Prof. Chao Yu

E-mail: yuchaom@163.com

Phone: (86) 23-68485378

Fax: (86) 23-68485161

Full address: Box 380#, College of Pharmacy, Chongqing Medical University, 1 Yi Xue Yuan Road, Chongqing 400016, P. R. China.

ABSTRACT

We are presenting an electrochemical immunosensor for the determination of Galectin-3 (Gal-3), a biomarker of heart failure. A glassy carbon electrode (GCE) was modified with a film of a composite made from the N-doped graphene nanoribbons immobilized Fe-based-Metal-organic frameworks deposited with Au nanoparticles (N-GNRs-Fe-MOFs@AuNPs). Primary antibody against Gal-3 (Gal-3-Ab_1) was immobilized on the Au nanoparticles on the surface of the modified GCE which then was blocked with bovine serum albumin. Signal amplification is crucial for obtaining low detection limits in biosensors. Here, a relatively simple and ultrasensitive sandwich-type electrochemical immunosensor based on novel signal generation and amplification was developed for the determination of Gal-3. A kind of novel redox-active species, AuPt-Methylene blue (MB) (AuPt-MB) nanocomposites, was synthesized by a one-pot method for the first time. Wherein, MB as a kind of the electron transfer mediators in an amperometric biosensor is responsible for electron production and signal amplification. The rod-like AuPt-MB nanohybrids displayed uniform morphology and good electrochemical activity and can combine with the second antibodies against Gal-3 (Gal-3-Ab_2). And the AuPt-MB-Ab_2 coupled with the N-GNRs-Fe-MOFs@AuNPs-Ab_1 to form the sandwich type format that can greatly enhance the biosensor's sensitivity. Under optimal conditions, the designed immunosensor exhibited a linear concentration range from 100 fg mL^{-1} to 50 ng mL^{-1}, with a low detection limit of 33.33 fg mL^{-1} (S/N=3) for Gal-3 in spiked serum. Additionally, the designed immunosensor showed acceptable selectivity, reproducibility and stability. The satisfactory results in analyzing human serum samples indicated potential application promising in monitoring biomarkers.

Keywords: galectin-3; sandwich-type electrochemical immunosensor; AuPt-Methylene blue; N-doped graphene nanoribbons; Fe-MOFs

1. Introduction

Elevated levels of galectin-3 have been found to be significantly associated with higher risk of death in both acute decompensated heart failure and chronic heart failure populations (Meijers et al.,2016; Mueller and Dieplinger,2016; Polat et al.,2016). Monitoring the Gal-3 changes in serum is notably important to predict the progression of the cardiovascular risk. The traditional assay methods of Gal-3 mainly are enzyme-linked immunosorbent assay (ELISA) (Eliaz et al.,2017; Polat et al.,2016; van Boxtel et al.,2015), immunohistochemical (Coppin et al.,2016; Raspollini et al.,2016) and the "routine Gal-3" assay (Abbott Diagnostics) (Mueller et al.,2016). Although these methods exhibit high sensitivity and selectivity, these traditional assays still need to be improved, such as time-consuming, the dependence of sophisticated and expensive equipment and requiring the skillful operator. (Zhang et al.,2015). In particular, they cannot meet the clinical demand of early-stage detection. Thus, facile and sensitive assays for Gal-3 detection are highly desirable. The electrochemical immunosensor with significant advantages of low detection limits, high sensitivity, ease of operation and low manufacturing cost (Feng et al.,2017), as promising method has been widely applied in detection of the clinical biomarker.

Methylene blue (MB), as a kind of electrochemical redox-active species (Dutta et al.,2017; Tang et al.,2017), owing to the presence of electron rich sulphur and nitrogen heteroatoms in their structure (Manasa et al.,2017), was usually applied in fabrication of electrochemical sensor. However, the application of MB in immunosensing is limited by its inhomogeneous morphology (Shan et al.,2016). To address this issue, Tang et al had designed a nanohybrids of Au-poly(MB) with characteristics of uniform morphology and innate strong redox peak current (Tang et al.,2017). Compared with the corresponding monometallic nanoparticles, bimetallic nanoparticles possessed many favorable characteristics including increased surface area, improved electron transfer rate, enhanced biocompatibility and promoted stability, due to the synergistic effects of these two monometallic nanoparticles (Zhao et al.,2015). Inspired by these remarkable advantages of bimetallic nanoparticles, the

AuPt-MB nanocomposites were designed and synthesized in this work for the first time. Surprisingly, the rod-like AuPt-MB nanocomposites synthesized firstly by our team, not only exhibited good uniform morphology but also showed outstanding electrochemical activity. The rod-like AuPt-MB nanocomposites were employed for signal generation and amplification as a new redox sandwich type nanoprobe in the present work.

To improve the stability and the sensitivity of this electrochemical immunosensor, the N-doped graphene nanoribbons immobilized Fe-based-Metal-organic frameworks deposited with Au nanoparticles (N-GNRs-Fe-MOFs@AuNPs) nanohybrids were combined as substrate matrix in this strategy. Wherein, the metal organic frameworks (MOFs) was a type of zeolite-like crystalline porous materials (Xie et al.,2015), featuring large surface area, flexible porosity and active sites (Wang et al.,2017b). As a new versatile material, MOFs have been widely implicated to gas storage/separation (Li et al.,2014), catalysis (Liu and Li,2016) and sensing (Zhan et al.,2013). In this work, Fe-based-Metal-organic frameworks (Fe-MOFs) with high stability and large surface area were synthesized by a facile method. Due to the large surface area, they can decorate with a large number of AuNPs *via* Au-N bonds to enhance the electrical conductivity of Fe-MOFs and immobilize more primary antibodies (Ab_1) via the interaction of Au-NH_2 in the next step. In order to further increase the conductivity of the substrate matrix, N-doped graphene nanoribbons (N-GNRs) were employed to hybrid with the Fe-MOFs@AuNPs. N-GNRs were synthesized from N-doped multiwalled carbon nanotubes (N-MWCNTs) which were widely employed to improve the conductivity performances of the surface of the modified electrodes (Fusco et al.,2017). Compared with carbon nanotubes, N-GNRs possess enhanced chemical activity and adsorption, due to the reactive edges, inherent terraces and step structures (Li et al.,2015b). Interestingly, the nanohybrids of N-GNRs-Fe-MOFs@AuNPs as the substrate material in this study not only take the advantages of the both N-GNRs and Fe-MOFs@AuNPs, but also have shown a remarkable synergistic effect for improving the performance of this immunosensor.

In this work, a novel sandwich-type immunosensor was fabricated successfully

basing on N-GNRs-Fe-MOFs@AuNPs as the substrate platform and AuPt-MB as a new redox nanoprobe for the generation and amplification of electrochemical signal for the first time. The application of N-GNRs-Fe-MOFs@AuNPs not only provided a good deal of active sites for the immobilization of primary antibody but also accelerated the electron transfer rate to improve the sensitivity of this immunosensor. Meanwhile, AuPt-MB nanohybrids have taken the advantages of the AuPt bimetallic nanoparticles to amplify its electrochemical signal and immobilize the second antibodies against Gal-3. The designed strategy has showed high sensitivity and excellent stability for quantitative determination of Gal-3 and can also be applied to the detection of other proteins.

2. Experimental

2.1. Materials and chemicals

Galectin-3 (Gal-3), galectin-3-Ab_1 (Gal-3-Ab_1) and galectin-3-Ab_2 (Gal-3-Ab_2) were purchased from Cloud-Clone Corp. (St. Houston, USA, www. cloud-clone.com). Dopamine (DA), L-threonine, dodecyltrimethylammonium bromide (DTAB) and glucose were purchased from Aladdin (Shanghai, China, www.aladdin-e.com). N-doped multiwalled carbon nanotubes (N-MWCNTs) were obtained from Xfnano, Inc (NanJing, China, www. Xfnano.com). Gold (III) chloride trihydrate ($HAuCl_4 \cdot 4H_2O$), chloroplatinic acid (H_2PtCl_6), dimethylformamide (DMF), methylene blue (MB) and 2-aminoterephthalic acid were obtained from Sigma-Aldrich (St. Louis, USA, www.sigmaaldrich.com). Bovine serum albumin (BSA), potassium ferricyanide ($K_3Fe(CN)_6$) and potassium ferrocyanide ($K_4Fe(CN)_6$) were provided by Beijing Chemical Reagents Company (Beijing, China). $FeCl_3 \cdot 6H_2O$, $NaBH_4$, and acetic acid were purchased from Chongqing Chuandong Chemical Group Co., Ltd (Chongqing, China). Healthy human serums were obtained from the First Affiliated Hospital of Chongqing Medical University (Chongqing, China). 0.1 M phosphate buffer saline (PBS) with different pH value were prepared by mixing

H_3PO_4, NaOH and KCl. All other reagents were of analytical reagent grade and used without further purification. Ultrapure water (> 18.2 MΩ) obtained from a Millipore Mill-Q purification system was used throughout the experiment.

2.2. Apparatus and measurements

The images of different nanomaterials were characterized by field emission scanning electron microscopy (FE-SEM, JEOL JSM-6700F, Japan) and transmission electron microscopy (TEM, Hitachi-7500158). Energy dispersive X-ray spectroscopy (EDS) was scaled using a JEOL JSM-6700F microscope (Japan). Atomic force microscopy (AFM) images were monitored by Bruker Dimension icon (USA). All electrochemical experiments were performed with a CHI660D electrochemical workstation (Chenhua Instruments Co., Shanghai, China) at room temperature using a conventional three-electrode system composed of a modified glassy carbon electrode (GCE, 4 mm in diameter) as a working electrode, a saturated calomel electrode (SCE) as the reference electrode and a platinum wire as an auxiliary electrode.

2.2. Preparation of N-GNRs and N-GNRs-Fe-MOFs@AuNPs

N-GNRs were synthesized by a modified method according to references (Li et al.,2015b). In brief, N-MWCNTs (0.05 g) were mixed with H_2SO_4 and H_3PO_4 at the ratio of 9:1 and heated at 140 °C for 10 min in an autoclave under magnetic stirring. After added $KMnO_4$ (0.25 g), the solutions were transferred into an oil bath at 65 °C for 8 min. Following the centrifugal separation process, the N-GNRs were obtained after washed three times with ultrapure water and dried under vacuum condition.

Fe-MOFs were prepared based on our previous work (Chen et al.,2017). 0.692 mM (0.187 g) of $FeCl_3 \cdot 6H_2O$ and 0.692 mM (0.126 g) of 2-aminoterephthalic acid were dissolved in 15 mL of DMF. The mixture solution was then placed in a silicone oil bath at 120 °C for 4 h, and 3.45 mM acetic acid was added to this solution after heating for 15 min. Following slow cooling to room temperature, the obtained

Fe-MOFs were isolated by centrifugation and washed with DMF, ethanol and ultrapure water to remove surplus reactants. Finally, the precipitate was dried in a vacuum oven overnight. Fe-MOFs@AuNPs was synthesized by using the $NaBH_4$ reduction method. Typically, 1 mL of $HAuCl_4$ (1 wt%) was added into 1 mL of prepared Fe-MOFs solution (1 mg mL^{-1}) and vigorously sonicated for 20 min. Subsequently, 2 mL of $NaBH_4$ (0.1 M) solution was added dropwise to the mixture with stirring for 30 min. Then, the mixture was isolated by centrifugation and washed with ultrapure water three times.

In the process of preparation N-GNRs-Fe-MOFs@AuNPs (Scheme 1A), a mixture solution of N-GNRs(1 mg mL^{-1}, 1 mL) and Fe-MOFs@AuNPs (1 mg mL^{-1}, 2 mL) was sonicated for 30 min and stirred for 12 h at room temperature, followed by centrifugation and washing with ultrapure water. Ultimately, the composites were dispersed again in 2 mL deionized water and kept at 4 °C for the following experiments.

2.3. Preparation of AuPt-MB and AuPt-MB-Ab_2

AuPt-MB was synthesized by a modified method according to the literature (Shan et al.,2016). HCl (0.1 M, 600 μL) and DTAB (1.14 mM, 6 mL) were added to 1 mL of MB solution (9.8 mM), and then micelles were formed after vigorously stirring for 10 min. Subsequently, $HAuCl_4$ (4 wt%, 100 μL) and H_2PtCl_6 (4 wt%, 100 μL) were added into the mixture at a time and continually agitated for 6 h at room temperature. Then, the composites were centrifuged at 8000 rpm about 10 min and were washed with ultrapure water for several times. Finally, the composites were redispersed in 2 mL 0.1 M PBS (pH 7.0) and then restored in 4°C prior to use.

The preparation procedure of AuPt-MB-Ab_2 is presented in Scheme 1B. 100 μL Gal-3-Ab_2 was added into 2 mL of prepared AuPt-MB composites solution and gently stirred for about 12 h at 4 °C. For fear of nonspecific adsorption, 40 μL BSA (1 wt%) was mixed with the bioconjugates for about 6 h at 4 °C after incubation. Eventually, the probes were centrifuged and redispersed in 0.1 M PBS (pH 7.0) and then restored

in 4°C before use.

2.4. Fabrication of the sandwich-type electrochemical immunosensor

The process of the construction of the sandwich type electrochemical immunosensor was shown in Scheme 1. Generally, the glassy carbon electrode (GCE) was polished by alumina polishing powders with the particle size of 0.3 and 0.05 μm, respectively. After washing ultrasonically in ultrapure water, absolute alcohol and ultrapure water successively, the electrode was dried at room temperature. Then, 10 μL of N-GNRs-Fe-MOFs@AuNPs suspension was dropped on the cleaned GCE and dried at room temperature. After that, 6 μL of Gal-3-Ab_2 dispersion (25 μg mL^{-1}) was loaded on the N-GNRs-Fe-MOFs@AuNPs-modified GCE and incubated for 12 h at 4 °C to anchor the antibody to the surface of electrode. After washing thoroughly, the electrode was blocked with BSA solution (1 wt%) for 30 min at room temperature to eliminate nonspecific binding sites between the analytes and electrode. Then, 6 μL of Gal-3 solution with a series of concentrations was added onto electrode surface and incubated for 1 h at 37 °C. Finally, 10 μL of AuPt-MB-Ab_2 solution was coated on the electrodes for 1 h at 37 °C. After rinsing, the prepared electrodes were fabricated successfully and stored at 4 °C when not in use.

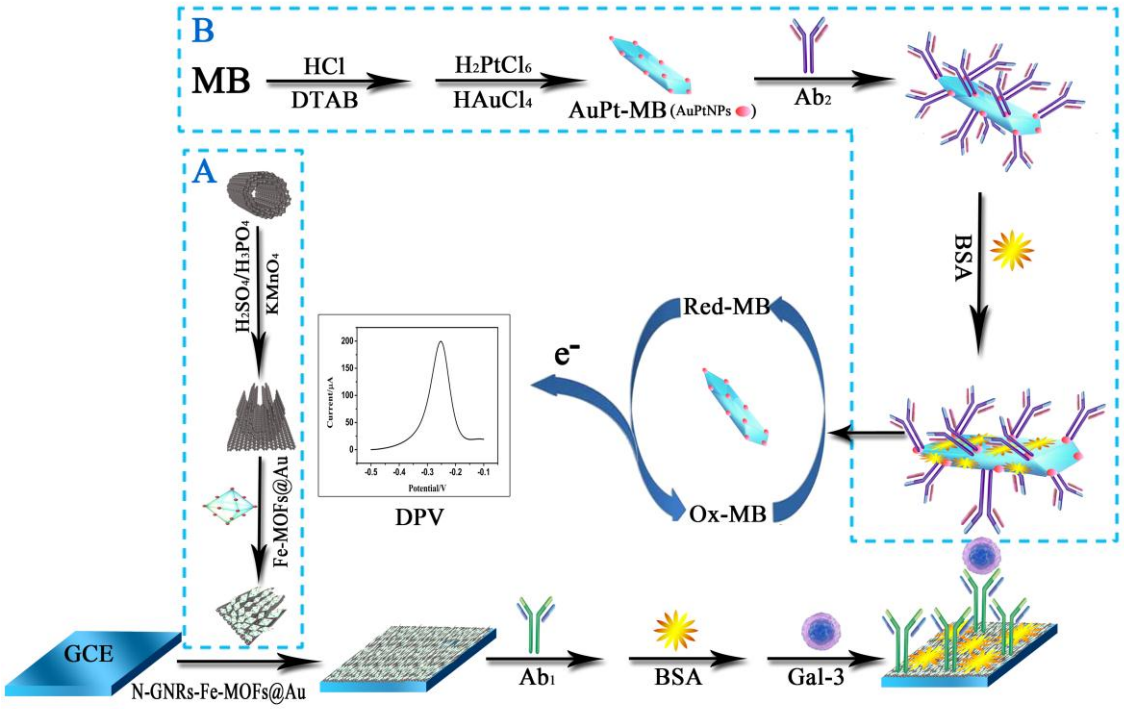

Scheme 1. Schematic illustration of the stepwise assembly procedure of the electrochemical immunosensor interfaces. The preparation procedures of (A) N-GNRs-Fe-MOFs@AuNPs and (B) AuPt-MB-Ab_2 bioconjugates.

2.5. Measurement procedure

Differential pulse voltammetry (DPV) was used to measure the electrochemical characteristics of the prepared electrodes. The DPV scan was performed from -0.5 V to -0.1 V with pulse amplitude of 50 mV, pulse width of 50 ms and pulse period of 100 ms in 5.0 mL of PBS (0.1 M, pH 7.0). The cyclic voltammetry (CV) experiments were performed in the solution containing 5 mmol L^{-1} $K_3[Fe(CN)_6]$ and 0.1 mmol L^{-1} KCl by scanning the potential from -0.2 V to 0.6 V and the scan rate was chosen as 50 mV s^{-1}. All electrochemical measurements were conducted at room temperature.

3. Results and discussion

3.1. Characterization of different nanomaterials

TEM and FE-SEM were used to illustrate the size and morphology of the as-prepared nanomaterials. As shown in Fig. 1A, the N-GNRs with diameters of approximately 100 nm and variable thickness. Compared with N-MWCNTs (Fig. S1A), the N-GNRs turned to be the partially unzipped nanotubes, which were similar to the previous report (Li et al.,2015b). Fig. 1B displays clearly the regular octahedron figure of the Fe-MOFs with an average diameter of 100 nm approximately, which was consistent with our previous work (Chen et al.,2017). After the Fe-MOFs was treated by $HAuCl_4$ and $NaBH_4$, a large amount of Au nanoparticles were clearly observed on the Fe-MOFs surface (Fig. 1C), indicating that the Fe-MOFs@AuNPs composites were synthesized successfully. In order to further confirm the Fe-MOFs@AuNPs composites, EDS was employed to analyze the chemical composition of the Fe-MOFs@AuNPs, the observed elements of Fe, N, C, N and O implying the successful synthesis of the Fe-MOFs@AuNPs (Fig. S1B). As shown in Fig. 1D, there was a large amount of Fe-MOFs@AuNPs loaded on the surface of N-GNRs evenly, which clearly confirmed the successful synthesis of N-GNRs-Fe-MOFs@AuNPs. As shown in Fig. 1E, the as-prepared AuPt-MB was micron-sized and stick-like nanocomposites with good uniform morphology. EDS was employed to further analyze the chemical composition of the AuPt-MB composites (Fig. 1F), and characteristic elements of Pt, Au, C, N, S and Cl could be observed, implying the successful synthesis of AuPt-MB.

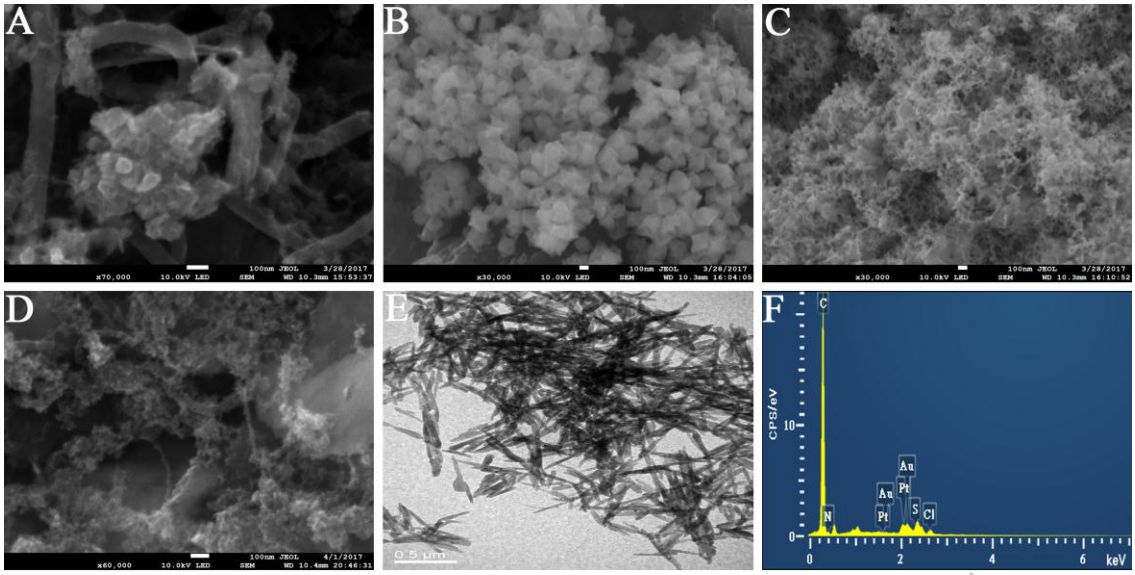

Fig. 1. FE-SEM images of (A) N-GNRs, (B) Fe-MOFs, (C) Fe-MOFs@AuNPs, (D) N-GNRs-Fe-MOFs@AuNPs and (E) TEM image of AuPt-MB. (F) EDS of AuPt-MB.

3.2. Characteristics of the immunosensor fabrication

CV was regarded as a convenient and effective method for probing the interface properties of surface-modified electrodes during the process of fabrication (Li et al.,2017). As shown in Fig. 2A, when the surface of bare GCE was coated with N-GNRs-Fe-MOFs@AuNPs, the redox peak current was obviously increased (curve b) compared with bare GCE (curve a), due to the excellent conductivity of N-GNRs-Fe-MOFs@AuNPs. However, the redox peak current was decreased orderly when the modified electrode was combined with Gal-3-Ab_1 (curve c), BSA (curve d) and the target (curve e), because of the bioactive substances greatly inhibited the efficiency of electron transfer. In summary, the fabrication of immunosensor was successful.

For further verification of successful fabrication of the immunosensor, atomic force microscopy (AFM) was used to monitor the changes of the surface features during the fabrication process of this immunosensor. As shown in Fig. S2, after combination with Gal-3-Ab_1 (Fig. S2B), the height of surface was increased with increased roughness compared with the N-GNRs-Fe-MOFs@AuNPs modified

electrode (Fig. S2A). After BSA was coated onto the electrode to block the non-specific binding sites, the surface became relatively smooth and the height was comparatively constant (Fig. S2C). Finally, when the target of Gal-3 was specifically binded with the galectin-3-Ab_1, the height and roughness of the surface were both increased significantly (Fig. S2D). Therefore, both of the CV and AFM can demonstrate that the immunosensor was fabricated successfully.

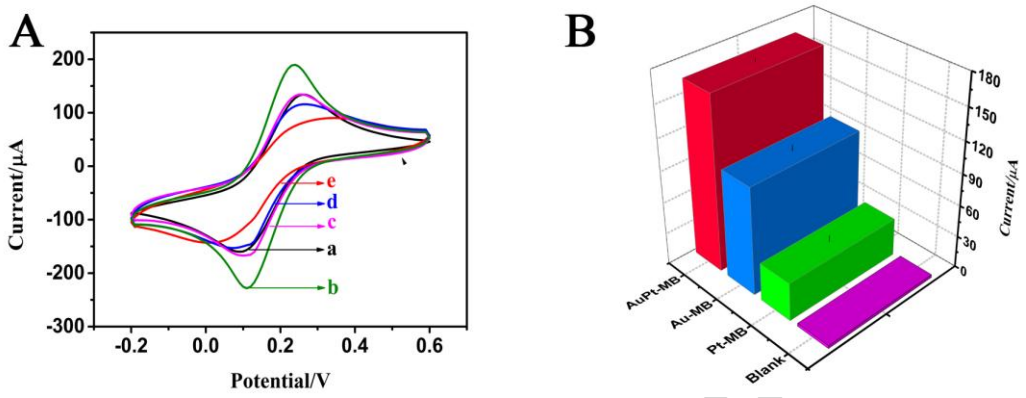

Fig. 2. (A) Typical CV studies of (a) bare GCE , (b) GCE/N-GNRs-Fe-MOFs@AuNPs, (c) GCE/N-GNRs-Fe-MOFs@AuNPs/Ab_1 , (d) GCE/N-GNRs-Fe-MOFs@AuNPs/Ab_1/BSA and (e) GCE/N-GNRs-Fe-MOFs@AuNPs/Ab_1/BSA/Gal-3 in 5 mmol L^{-1} $K_3[Fe(CN)_6]$ and 0.1 mmol L^{-1} KCl. (B) The DPV current responses of the immunosensor incubated with different redox nanoprobe materials.

3.3. Synergistic effect and stability of N-GNRs-Fe-MOFs@AuNPs nanohybrids

To confirm that the N-GNRs-Fe-MOFs@AuNPs nanocomposites as the substrate matrix was our best choice, the synergistic effect of N-GNRs-Fe-MOFs@AuNPs nanocomposites was investigated by DPV in 5 mmol L^{-1} $K_3[Fe(CN)_6]$ and 0.1 mmol L^{-1} KCl. The results are shown in detail in the Supplementary Information S1 (Fig. S3).

The stability of the N-GNRs-Fe-MOFs@AuNPs nanocomposites was aso verified by CV for running 50 circles. The results are shown in detail in the Supplementary Information S2 (Fig. S4).

3.4. Comparison of different signal amplification strategies

In order to demonstrate the effect of AuPt-MB, we have made the comparison of different signal amplification strategies of Pt-MB-Ab_2, Au-MB-Ab_2 and AuPt-MB-Ab_2. All of the assay procedures were implemented with the same concentration of target Gal-3 (1.25 ng mL^{-1}) and incubated with different signal nanoprobes of Pt-MB-Ab_2, Au-MB-Ab_2 and AuPt-MB-Ab_2 respectively, and then tested by DPV. As shown in Fig. 2B, compared with the blank group, the immunosensor which incubated with Pt-MB-Ab_2 showed a clear current response, because Pt-MB-Ab_2 acted as redox nanoprobe generating the electrochemical signal. Compared with the Pt-MB-Ab_2, the current response increased when using Au-MB-Ab_2 as redox nanoprobe, owing to the electron transfer ability of Au-MB is stronger than Pt-MB. Notably, the current increased much higher than that of Pt-MB-Ab_2 and Au-MB-Ab_2 when the immunosensor was incubated with AuPt-MB-Ab_2. This interesting phenomenon indicated the remarkable advantages of bimetallic nanoparticles compared to the corresponding monometallic nanoparticles. By studying comparatively, the AuPt-MB is superior to the corresponding monometallic materials as a label in the amplification of the analytical signal.

3.5. Optimization of experimental conditions

The electrochemical properties of the immunosensor are influenced by many factors. In order to achieve optimal immunoassay performance, several conditions were selected to investigate, such as pH value, the volume of substrate material solution, the immobilization time of Gal-3-Ab_1 and the incubation time of Gal-3. Various working electrodes have been used to detect Gal-3 (1 ng mL^{-1}) in different conditions.

The pH of the PBS has a great influence on the immunosensor. Fig. S5A displays the effect of the pH value of PBS on the current response. The current signal increased with the variation of pH from 6.0 to 7.0, and then decreased with the further

pH increase from 7.0 to 8.0, because the high alkaline may damage the activity of biomolecules and break the linkage of antigen-antibody (Li et al.,2015a). The largest electrochemical signal was achieved at pH value of 7.0. Therefore, pH 7.0 PBS (0.1 M) was selected as the optimal detection solution for further experiments.

The volume of N-GNRs-Fe-MOFs@AuNPs nanocomposites was investigated to improve the sensitivity of the immunosensor and provide a favorable platform for immobilizing galectin-3-Ab_1. As shown in Fig. S5B, the current response increased rapidly with the increasing volume from 6 μL to 10 μL, and then the current change decreased when the volume become higher than 10 μL. The current variations indicated that the appropriate volume of N-GNRs-Fe-MOFs@AuNPs efficiently enhanced the electron conductivity; but in high volume, the excessively thick film of N-GNRs-Fe-MOFs@AuNPs could hinder the electron transfer because of the increased interface resistance. Therefore, 10 μL was chosen as the optimal volume of N-GNRs-Fe-MOFs@AuNPs.

In addition, to achieve an optimal electrochemical signal, the immobilization time of galectin-3-Ab_1 was tested. As shown in Fig. S5C, with the increase of immobilization time, the current responses of the immunosensor was first increased and then remained steady at approximately 10 h, demonstrating that the optimal immobilization time of galectin-3-Ab_1 was obtained. Therefore, 10 h was chosen as the immobilization time of galectin-3-Ab_1.

Furthermore, for recognition of Gal-3, incubation time is an extremely important parameter. A period of time is required for the Gal-3-Ab_1 to specifically bind the Gal-3. With an increase in incubation time, the current responses first increased and then remained stable at 60 min (Fig. S5D), indicating that the amount of Gal-3 captured on the sensor surface had reached maximum. Therefore, the optimal incubation time of Gal-3 was 60 min.

3.6. Analytical performance of the immunosensor

To evaluate the sensitivity and quantitative range of the prepared immunosensor,

we subjected it to various concentrations of the Gal-3 standard solution under the optimal detection conditions. As shown in Fig. 3A, the DPV current reponses of the immunosensor gradually increased with increasing concentrations of target Gal-3 in 5 mL of PBS (0.1 M, pH 7.0). Meanwhile, the calibration plot displayed a good linear relationship between the peak currents and the logarithm of target concentrations in the range of 100 fg mL^{-1} - 50 ng mL^{-1} with the detection limit of 33.33 fg mL^{-1} (S/N = 3); the linear regression equation was DI (μA) = 154.37865 +20.45223logC (ng mL^{-1}) (n = 3, R = 0.99502) (Fig. 3B). Overall, this great performance is most likely due to the synergistic effect of the N-GNRs-Fe-MOFs@AuNPs, AuPt-MB and antigen-antibody specific binding. The excellent electrical conductivity and the large electroactive surface of N-GNRs-Fe-MOFs@AuNPs promoted the electron transfer; the large biocompatibility bimetallic nanoparticles of AuPt hybridized with MB could result in a high loading of galectin-3-Ab_2, promoting of the sensitivity and amplification of the immunosensor. Compared with the other methods such as ELISA (Table.S1) and electrochemical biosensors in previous reports (Table.S2), the developed immunosensor showed lower detection limit and wider linear range. As a result, a novel and ultrasensitive immunosensor for Gal-3 detection was obtained.

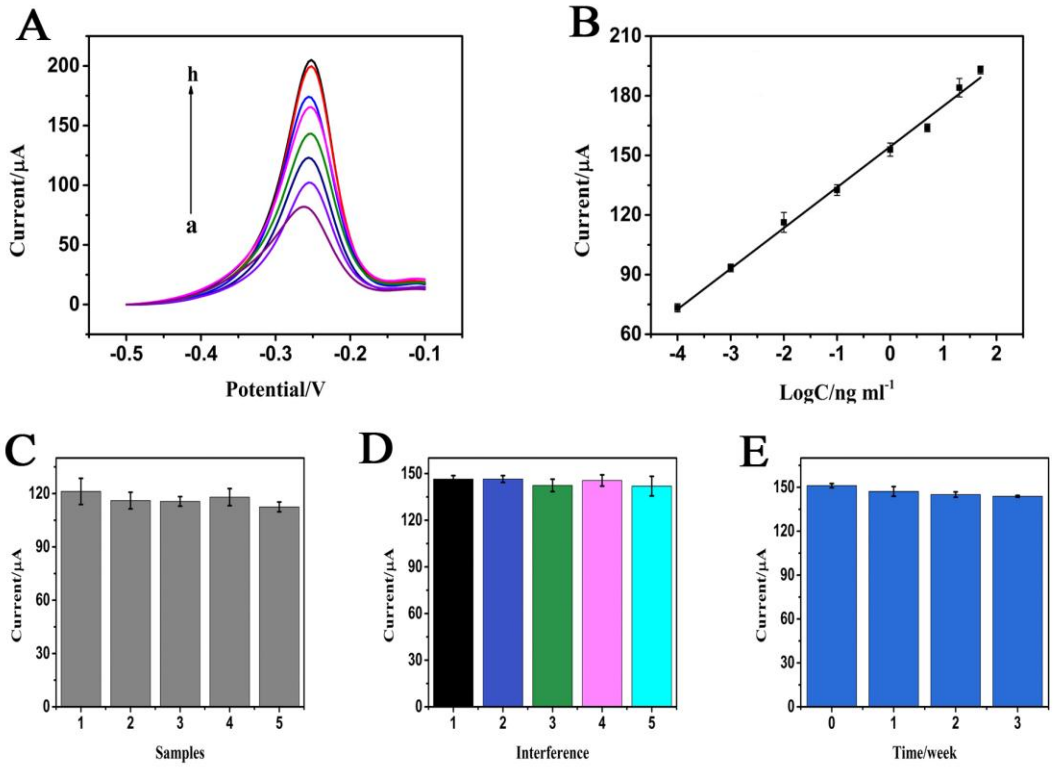

Fig. 3. (A) DPV responses of the proposed immunosensor after incubation with different Gal-3 concentrations (From a to h: 0.0001, 0.001, 0.01, 0.1, 1.0, 5.0, 20, 50 ng mL^{-1}) in 0.1M PBS (pH = 7.0) at a scan rate of 50 mV s^{-1} (vs. SCE); (B) Calibration plot of the developed immunosensor for Gal-3 (logC vs. peak current responses). The DPV response of prepared biosensor (C) five different electrodes treated in the same way (n=5 RSD=2.75%). (D) 1 ng mL^{-1} Gal-3 (1), 1 ng mL^{-1} Gal-3 + 100 ng mL^{-1} glucose (2), 1 ng mL^{-1} Gal-3 + 100 ng mL^{-1} Dopamine (3), 1 ng mL^{-1} Gal-3 + 100 ng mL^{-1} L-threonine (4), 1 ng mL^{-1} Gal-3 + 100 ng mL^{-1} BSA (5). (E) The stability study of the immunosensor.

3.7. Selectivity, stability and repeatability of the immunosensor

Selective determination of target analytes plays an important role in analyzing biological samples (Wang et al.,2017a). Interfering substances such as glucose, dopamine, L-threonine and BSA were used to confirm that the change in current was a result of the specific recognition of Gal-3. The Gal-3 solutions (1 ng mL^{-1}) containing interfering substances (100 ng mL^{-1}) were measured by the designed immunosensor and the results were shown in Fig. 3C. The current signal variation was 1.55%, indicating that the selectivity of the immunosensor is acceptable.

To evaluate the reproducibility of the proposed immunosensor, five working electrodes were prepared for the detection of Gal-3 (1 ng mL^{-1}) under the same conditions (Fig. 3D). The relative standard deviation (RSD) of the measurements for the five electrodes was 2.75%. The results indicated the proposed immunosensor displayed good precision and reproducibility.

The prepared biosensor was stored in a fridge at 4 °C. After storage for 3 weeks, the change in current retained 95.17% of its original current (Fig. 3E). The results indicated the proposed immunosensor possessed good stability.

3.8. Application for the analysis of serum samples

In order to assess the accuracy and the feasibility of the immunosensor for real sample analysis, the prepared immunosensor was used to detect the recoveries of Gal-3 in the serum sample by standard addition methods. The biosensor was applied

to human diluted serum samples spiked with 1ng mL $^{-1}$, 1.25ng mL $^{-1}$, 2.5ng mL^{-1} and 5ng mL $^{-1}$ Gal-3 solution, and the recoveries of the four concentrations were 104.84%, 102.7%, 97.99% and 98.91%, and the RSDs were 3.79%, 3.74%, 4.51% and 3.52%, respectively, suggesting acceptable precision(Table 1). To further validate the precision of the proposed immunosensor, human serum spiked samples with 1 ng mL $^{-1}$, 2.5 ng mL $^{-1}$, 6.5 ng mL $^{-1}$, 10 ng mL $^{-1}$ and 20 ng mL $^{-1}$ of Gal-3 were distributed into two aliquots and detected either using our immunosensor or the classical ELISA method (Fig. 4). The linear regression coefficient was 0.99941 and the slope of the immunosensor versus ELISA plot was 1.0194, demonstrating an excellent correlation between the results given by two methods. These results indicated that the proposed immunosensor represented satisfying accuracy. Therefore, the purposed immunosensor could be effectively applied to the quantitative detection of galectin-3 in human serum and also has the potential application promising in the monitoring of clinical protein biomarkers.

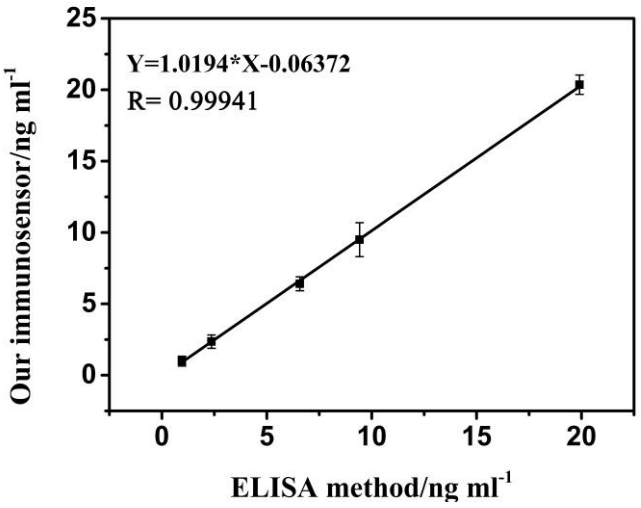

Fig. 4. Comparing the detection of Gal-3 spiked human serum samples by ELISA and our immunosensor

Table 1. Spike and recovery results (n = 3) obtained from the Gal-3 immunosensor inhuman plasma.

Samples	Added concentration (ng/ml)	measured concentration (ng/ml)	Recovery (%)	RSD (%)
Sample -1	1	0.99±0.055	104.84	3.79%
Sample -2	1.25	1.28±0.048	102.70	3.74%
Sample-3	2.5	2.45±0.110	97.99	4.51%
Sample-4	5	4.95±0.174	98.91	3.52%

4. Conclusion

In summary, a specific and sensitive sandwich-type electrochemical immunosensor for the detection of galectin-3 based on N-GNRs-Fe-MOFs@AuNPs and AuPt-MB nanocomposites was successfully developed. N-GNRs-Fe-MOFs@AuNPs as a substrate platform of the immunosensor has a large specific surface area and numerous active sites to capture primary antibodies and observably accelerate the electron transfer. Additionally, AuPt-MB as a new redox nanoprobe for the generation and amplification of electrochemical signal and can easily capture detection antibodies via Pt-NH_2 and Au-NH_2. Compared with the analysis performance of other methods, the purposed immunosensor exhibits higher sensitivity and a wider linear range for the detection of galectin-3. The designed immunosensor has displayed a linear response with high sensitivity, good reproducibility, favorable stability and excellent selectivity towards Gal-3, indicating a promising application in clinical diagnosis. However, the construction time of the whole sensor is a little long, so our further work is to shorten the construction time of the sensor to meet the requirements of bedside detection of clinical markers.

Acknowledgment

We are grateful for the financial support from the National Nature Science Foundation of China (No. 81370403), Chongqing foundation and advanced research project (No.

CSTC2015jcyjBX0053), Chongqing precision medical key technology research and development and demonstration projects (cstc2016shms-ztzx0042) and Chongqing medical university scientific research cultivating fund (No.201414).

Reference

Chen, J., Yu, C., Zhao, Y., Niu, Y., Zhang, L., Yu, Y., Wu, J., He, J., 2017. Biosens Bioelectron 91, 892-899.

Coppin, L., Benomar, K., Corfiotti, F., Cattan, S., Renaud, F., Lapere, C., Leteurtre, E., Vantyghem, M. C., Truant, S., Pigny, P., 2016. Pancreatology 16, 115-120.

Dutta, G., Nagarajan, S., Lapidus, L. J., Lillehoj, P. B., 2017. Biosens Bioelectron 92, 372-377.

Eliaz, I., Patil, A., Navarro-Alvarez, N., Wang, Z., Eliaz, A., Weil, E., Wilk, B., Sachs, D. H., Huang, C. A., 2017. J Clin Apher.

Feng, J., Li, Y., Li, M., Li, F., Han, J., Dong, Y., Chen, Z., Wang, P., Liu, H., Wei, Q., 2017. Biosens Bioelectron 91, 441-448.

Fusco, G., Gallo, F., Tortolini, C., Bollella, P., Ietto, F., De Mico, A., D'Annibale, A., Antiochia, R., Favero, G., Mazzei, F., 2017. Biosens Bioelectron 93, 52-56.

Li, B., Wen, H. M., Zhou, W., Chen, B., 2014. J Phys Chem Lett 5, 3468-3479.

Li, F., Han, J., Jiang, L., Wang, Y., Li, Y., Dong, Y., Wei, Q., 2015a. Biosens Bioelectron 68, 626-632.

Li, M., Wang, P., Li, F., Chu, Q., Li, Y., Dong, Y., 2017. Biosens Bioelectron 87, 752-759.

Li, N., Ma, H., Cao, W., Wu, D., Yan, T., Du, B., Wei, Q., 2015b. Biosens Bioelectron 74, 786-791.

Liu, M., Li, J., 2016. ACS Appl Mater Interfaces 8, 2158-2165.

Manasa, G., Mascarenhas, R. J., Satpati, A. K., D'Souza, O. J., Dhason, A., 2017. Mater Sci Eng C Mater Biol Appl 73, 552-561.

Meijers, W. C., van der Velde, A. R., de Boer, R. A., 2016. EJIFCC 27, 238-252.

Mueller, T., Dieplinger, B., 2016. EJIFCC 27, 224-237.

Mueller, T., Egger, M., Leitner, I., Gabriel, C., Haltmayer, M., Dieplinger, B., 2016. Clin Chim Acta 456, 19-23.

Polat, V., Bozcali, E., Uygun, T., Opan, S., Karakaya, O., 2016. Acta Cardiol 71, 191-197.

Raspollini, M. R., Luque, R. J., Menendez, C. L., Bollito, E., Brunelli, M., Martignoni, G., Montironi, R., Cheng, L., Blanca, A., Baroni, G., Minervini, A., Lopez-Beltran, A., 2016. Hum Pathol 57, 78-84.

Shan, J., Wang, L., Ma, Z., 2016. Sensors and Actuators B: Chemical 237, 666-671.

Tang, Z., Wang, L., Ma, Z., 2017. Biosens Bioelectron 92, 577-582.

van Boxtel, W., Bulten, B. F., Mavinkurve-Groothuis, A. M., Bellersen, L., Mandigers, C. M., Joosten, L. A., Kapusta, L., de Geus-Oei, L. F., van Laarhoven, H. W., 2015. Biomarkers 20, 143-148.

Wang, P., Li, M., Pei, F., Li, Y., Liu, Q., Dong, Y., Chu, Q., Zhu, H., 2017a. Biosens Bioelectron 91, 424-430.

Wang, Z., Yan, Z., Wang, F., Cai, J., Guo, L., Su, J., Liu, Y., 2017b. Biosens Bioelectron 97, 107-114.

Xie, S., Ye, J., Yuan, Y., Chai, Y., Yuan, R., 2015. Nanoscale 7, 18232-18238.

Zhan, W. W., Kuang, Q., Zhou, J. Z., Kong, X. J., Xie, Z. X., Zheng, L. S., 2013. J Am Chem Soc 135, 1926-1933.

Zhang, J., He, J., Xu, W., Gao, L., Guo, Y., Li, W., Yu, C., 2015. Electrochimica Acta 156, 45-52.

Zhao, Z., Zhang, M., Chen, X., Li, Y., Wang, J., 2015. Sensors (Basel) 15, 16614-16631.

Highlights

1. A novel sandwich-type electrochemical immunosensor for the detection of galectin-3 was designed at the first time.
2. The N-GNRs-Fe-MOF@AuNPs was first used in the immunosensor as substrate platform.
3. AuPt-MB was first synthesized and applied as signal probe.